Vilnius
University
Press

Spatiotemporal dynamics of a diffusive nutrient-phytoplankton model with delayed nutrient recycling[*]

Yun Yang, Yanfei Du[1]

School of Mathematics and Data Science,
Shaanxi University of Science and Technology,
Xi'an 710021, China
duyanfei@sust.edu.cn

Abstract. In this paper, we investigate the spatiotemporal dynamics of a diffusive nutrient-phytoplankton model with delayed nutrient recycling. We first study the stability of positive equilibrium and Turing instability induced by diffusion. We then investigate the effect of delay, and it turns out that the value of the rate of recycling k plays an important role in the Hopf bifurcation induced by delay. The delay will and will not induce Hopf bifurcation with low and high level of k, respectively. To reveal the spatiotemporal dynamics, Turing–Hopf bifurcation is carried out, and normal form is derived. Many spatiotemporal dynamics are found, including the coexistence of two stable spatially inhomogeneous periodic solutions or two stable spatially inhomogeneous steady-state solutions.

Keywords: plankton, diffusion, nutrient recycling delay, Turing–Hopf bifurcation, spatiotemporal dynamics.

1 Introduction

Plankton form the base of all food chains in the ocean and lakes, and phytoplankton are in the first trophic level. Moreover, phytoplankton produce oxygen for human life and other living animals and absorb almost half of the carbon dioxide, which may be contributing to global warming [2, 10]. However, a rapid increase or decrease of phytoplankton populations, which is known as "bloom", has adverse effects on aquatic population, ecosystem, and human health [2, 3, 17].

It has been widely recognized that one of the factors that contributes to algal blooming is eutrophication, which refers to the enrichment of waters by inorganic plant nutrients. Since the pioneering work of Riley et al. [20], the interaction of nutrient and plankton

has been extensively investigated through mathematical models [5,14]. Many experimental observations show that toxin producing phytoplankton (TPP) also play a role in the outbreak of phytoplankton blooms [8, 18, 24, 31, 34].

In nature, the portion of dead phytoplankton regenerates to the nutrient concentration due to bacterial decomposition. The effect of nutrient recycling on the stability of ecological systems has been widely studied [6,19]. Chakraborty et al. [6] proposed the following nutrient-phytoplankton model:

$$
\frac{\mathrm{d}N}{\mathrm{d}t} = a - bNP - eN + kP,
$$
$$
\frac{\mathrm{d}P}{\mathrm{d}t} = cNP - dP - \frac{\theta P^2}{\mu^2 + P^2},
$$

where N and P are the concentration of nutrient and the abundance of phytoplankton, respectively; a is the rate of constant external nutrient input into the system; b is the maximal nutrient uptake rate of phytoplankton, and c is the maximal conversion rate of nutrient into phytoplankton, where $c \leqslant b$; d is the per capita-mortality rate of phytoplankton, k is the portion of the phytoplankton recycled back to the nutrient concentration, where $k < d$; e is the per capital-loss rate of nutrient. θ represents the rate of release of toxic chemicals by the toxin-producing phytoplankton (TPP) population, and μ denotes the half-saturation constant. In [6], numerical simulations show the existence of the limit cycle, which indicates recurring blooms.

In lakes or oceans, current or turbulent lateral diffusion can lead to the movement of plankton population [7, 32]. Therefore, it is more realistic to take spatial diffusion into account when we model the nutrient and phytoplankton interaction. In fact, nutrient recycling after the death of plankton is not instantaneous, but it takes time to transform dead plankton to nutrient via bacterial decomposition [4, 13, 15, 23, 30]. Delayed nutrient recycling was first modeled by Beretta et al. [4] with a distributed delay. He and Ruan [13] used a distributed delay to describe nutrient recycling and a discrete delay to model the planktonic growth response to nutrient uptake, and they obtain some sufficient conditions for the global attractivity of the positive equilibrium. Motivated by [6] and the previous work, we consider a diffusive nutrient-phytoplankton model with delayed nutrient recycling

$$
\begin{aligned}
\frac{\partial N(x,t)}{\partial t} &= d_1 \Delta N(x,t) + a - bN(x,t)P(x,t) - eN(x,t) \\
&\quad + kP(x,t-\tau), \quad x \in (0,l\pi),\ t > 0, \\
\frac{\partial P(x,t)}{\partial t} &= d_2 \Delta P(x,t) + cN(x,t)P(x,t) - dP(x,t) - \frac{\theta P(x,t)^2}{\mu^2 + P(x,t)^2}, \\
&\quad x \in (0,l\pi),\ t > 0, \\
\frac{\partial N(x,t)}{\partial n} &= \frac{\partial P(x,t)}{\partial n} = 0, \quad x = 0,\ l\pi, t > 0, \\
N(x,t) &= N_0(x,t) \geqslant 0, \quad x \in (0,l\pi),\ -\tau \leqslant t \leqslant 0, \\
P(x,t) &= P_0(x,t) \geqslant 0, \quad x \in (0,l\pi),\ -\tau \leqslant t \leqslant 0,
\end{aligned}
\tag{1}
$$

where d_1 and d_2 are the diffusion coefficients of nutrient and phytoplankton, respectively, and τ is the nutrient recycling delay. Zhuang et al. [35] investigated Hopf bifurcation induced by nutrient recycling delay.

There have been many papers published on nutrient-phytoplankton models incorporating diffusion. Chakraborty et al. [7] investigated the spatial dynamics of a nutrient-phytoplankton system with toxic effect on phytoplankton. They obtained the condition for Turing instability and found that the distribution of nutrient and phytoplankton becomes inhomogeneous in space and results in different patterns, like stripes, spots, and the mixture of them depending on the toxicity level. Ruan [23] proposed a reaction-diffusion nutrient-plankton model with delayed growth response and delayed nutrient recycling and proved that there is a family of travelling wave solutions. Dai et al. [9] studied a nutrient-phytoplankton model described by a couple of reaction-diffusion equations with delay, and they found that the delay cannot only induce instability of a positive equilibrium, but also promote the formation of patchiness (an irregular pattern) via Hopf bifurcation. In addition, the numerical analysis indicated that eutrophic conditions may be a significant reason inducing phytoplankton blooms. Sigh el al. [25] discussed a model for interacting nutrient phytoplankton systems with the effect of toxic chemicals released by phytoplankton and time delay in toxin liberation. They observed that increasing values of toxin release results in the system dynamics show stable and oscillatory behavior without diffusion, and the time delay in toxin distribution term stabilizes and destabilizes the system dynamics. Tian and Zhang [29] explored the impact of time delay on spatiotemporal patterns in a plankton system, and they found that time delay can trigger the emergence of irregular spatial patterns via a Hopf bifurcation.

The aim of this paper is to investigate the joint effects of spatial diffusion and time delay on the spatiotemporal dynamics of the nutrient-phytoplankton system from the view of bifurcation analysis. First, we analyze diffusion-driven instability of the nondelayed system and give the conditions for the stability and Turing instability using diffusion coefficient as bifurcation parameter. Then we investigate the effect of nutrient recycling delay. Combining with numerical and analytical analysis, we find that the level of k plays an important role in Hopf bifurcation induced by τ. When the value of k is large, the delay τ does not induce instability to the positive equilibrium E^*, and Hopf bifurcation does not occur. When the value of k is small, τ may change the stability of E^* and induce Hopf bifurcation. Finally, to reveal the spatiotemporal dynamics induced by diffusion and delay, Turing–Hopf bifurcation analysis is carried out. We derive the normal form of Turing–Hopf bifurcation from which we can obtain the dynamical classification near Turing–Hopf bifurcation. Numerical simulations show complex dynamics, such as stable spatially homogeneous and inhomogeneous periodic solutions and nonconstant steady states.

The rest of this paper is organized as follows. In Section 2, we investigate the existence and stability of the equilibria and derive the conditions for Hopf bifurcation, Turing instability, and Turing–Hopf bifurcation. In Section 3, we derive the normal form of Turing–Hopf bifurcation. In Section 4, some numerical simulations are presented to verify the theoretical results, and the existence of stable spatially homogeneous and inhomogeneous periodic solutions as well as spatially inhomogeneous steady-state solutions are demonstrated. Finally, a brief conclusion is given in Section 5.

2   Local stability and bifurcation

In this section, we investigate the stability of equilibria and derive the conditions for bifurcations, including Turing bifurcation induced by diffusion, Hopf bifurcation induced by delay, and Turing–Hopf bifurcation.

2.1   Equilibria and local stability

In this subsection, we investigate the existence and stability of spatially homogeneous equilibria. Recall that we have assumed that $k < d$ and $c \leqslant b$, and therefore the following holds:

(H1) $bd - ck > 0$.

Firstly, we discuss the existence of equilibria. It is straightforward to see that model (1) always has an equilibrium $E_0 = (a/e, 0)$. Denote the positive equilibrium by $E^*(N^*, P^*)$, where $N^* = (a + kP^*)/(e + bP^*)$, and P^* is a positive root of the equation

$$h(P) := P^3 + v_1 P^2 + v_2 P + v_3 = 0$$

with

$$v_1 = \frac{b\theta - (ac - de)}{bd - ck}, \qquad v_2 = \frac{\theta e + (bd - ck)\mu^2}{bd - ck}, \qquad v_3 = \frac{-(ac - de)\mu^2}{bd - ck}. \quad (2)$$

Since we only consider spatially homogeneous equilibria, which are independed on space, thus we can discuss the existence of interior equilibria using the similar method in [6, 16]. We have the following results.

Lemma 1. *Suppose that* (H1) *holds, and* v_1, v_2 *and* v_3 *are defined in* (2).

   (i) *If* $ac - de \leqslant 0$, *system* (1) *has no positive equilibria.*
  (ii) *If* $0 < ac - de \leqslant b\theta$, *then system* (1) *has a unique positive equilibrium.*
 (iii) *Suppose that* $ac - de > b\theta$. *If* $v_1^2 - 3v_2 \leqslant 0$, *then system* (1) *has a unique positive equilibrium. If* $v_1^2 - 3v_2 > 0$, *system* (1) *has a unique positive equilibrium, provided* $h(P_-)h(P_+) > 0$; *system* (1) *has two positive equilibria, provided* $h(P_-)h(P_+) = 0$, *and three positive equilibria, provided* $h(P_-)h(P_+) < 0$, *where* $P_- = -v_1/3 - \sqrt{v_1^2 - 3v_2}/3$ *and* $P_+ = -v_1/3 + \sqrt{v_1^2 - 3v_2}/3$.

Now we consider the stability of the equilibrium E_0. The linearization of system (1) at E_0 is

$$\frac{\partial}{\partial t} \begin{pmatrix} N(x,t) \\ P(x,t) \end{pmatrix} = (D\Delta + L_1) \begin{pmatrix} N(x,t) \\ P(x,t) \end{pmatrix} + L_2 \begin{pmatrix} N(x,t-\tau) \\ P(x,t-\tau) \end{pmatrix}, \quad (3)$$

where

$$D = \begin{pmatrix} d_1 & 0 \\ 0 & d_2 \end{pmatrix}, \qquad L_1 = \begin{pmatrix} -e & -\frac{ab}{e} \\ 0 & \frac{ac}{e} - d \end{pmatrix}, \qquad L_2 = \begin{pmatrix} 0 & k \\ 0 & 0 \end{pmatrix}.$$

From [33] we know that the eigenvalue problem

$$-\Delta \xi = \sigma \xi, \quad x \in (0, l\pi), \qquad \xi'(0) = \xi'(l\pi) = 0$$

has eigenvalues $\sigma_n = n^2/l^2$, $n \in \mathbb{N}_0$, with corresponding normalized eigenfunctions

$$b_n(x) = \frac{\cos \frac{n}{l} x}{\| \cos \frac{n}{l} x \|} = \begin{cases} \sqrt{\frac{1}{l\pi}}, & n = 0, \\ \sqrt{\frac{2}{l\pi}} \cos \frac{n}{l} x, & n \geqslant 1. \end{cases}$$

The characteristic equation for linearized system (3) is

$$\det \left(\lambda I_2 + D \frac{n^2}{l^2} - L_1 - L_2 \mathrm{e}^{-\lambda \tau} \right) = 0,$$

where I_2 is the 2×2 identity matrix. It is equivalent to

$$\left(\lambda + d_1 \frac{n^2}{l^2} + e \right) \left(\lambda + d_2 \frac{n^2}{l^2} - \frac{ac}{e} + d \right) = 0,$$

and thus

$$\lambda_{1,n} = -d_1 \frac{n^2}{l^2} - e < 0, \qquad \lambda_{2,n} = -d_2 \frac{n^2}{l^2} + \frac{ac}{e} - d.$$

If $ac - de < 0$, we have $\lambda_{2,n} < 0$, and E_0 is locally asymptotically stable. If $ac - de > 0$, we have $\lambda_{2,0} > 0$, which implies that E_0 is unstable.

Lemma 2. *The equilibrium E_0 of system* (1) *is locally asymptotically stable if $ac - de < 0$, and it is unstable if $ac - de > 0$.*

In the rest of this paper, we only consider the case when system (1) has a unique positive equilibrium. Suppose

(i) $0 < ac - de \leqslant b\theta$;
(ii) $ac - de > b\theta$, $v_1^2 - 3v_2 \leqslant 0$;
(iii) $ac - de > b\theta$, $v_1^2 - 3v_2 > 0$, $h(P_-)h(P_+) > 0$.

Assume that

(H2) (i) or (ii) or (iii) holds.

Suppose that (H1) holds according to Lemma 1. We can get that system (1) has a unique positive equilibrium if (H2) holds.

The linearization of system (1) at E^* is

$$\frac{\partial}{\partial t} \begin{pmatrix} N(x,t) \\ P(x,t) \end{pmatrix} = (D\Delta + L_1') \begin{pmatrix} N(x,t) \\ P(x,t) \end{pmatrix} + L_2 \begin{pmatrix} N(x,t-\tau) \\ P(x,t-\tau) \end{pmatrix},$$

where

$$L_1' = \begin{pmatrix} l_{11} & l_{12} \\ l_{21} & l_{22} \end{pmatrix}, \qquad L_2 = \begin{pmatrix} 0 & k \\ 0 & 0 \end{pmatrix} \tag{4}$$

with $l_{11} = -bP^* - e < 0$, $l_{12} = -bN^* < 0$, $l_{21} = cP^* > 0$, $l_{22} = \theta P^*(P^{*2} - \mu^2)/$ $(\mu^2 + P^{*2})^2$. The corresponding characteristic equation is given by

$$\lambda^2 + A_n\lambda + B_n + Ce^{-\lambda\tau} = 0, \tag{5}$$

where $A_n = d_1 n^2/l^2 + d_2 n^2/l^2 - l_{11} - l_{22}$, $B_n = (d_1 n^2/l^2 - l_{11})(d_2 n^2/l^2 - l_{22}) - l_{12}l_{21}$, $C = -kl_{21} < 0$.

2.2 Turing instability for the nondelayed system

When $\tau = 0$, the characteristic equation (5) is transformed into the following equation:

$$\lambda^2 + A_n\lambda + B_n + C = 0, \ n \in \mathbb{N}_0. \tag{6}$$

Clearly, if $A_n > 0$, $B_n + C > 0$ for $n \in \mathbb{N}_0$, all roots of Eq. (6) have negative real roots. When $n = 0$, it corresponds to the case of temporal model without diffusion, which requires

(H3) $A_0 = -(l_{11} + l_{22}) > 0$, $B_0 + C = l_{11}l_{22} - (l_{12} + k)l_{21} > 0$

holding for the stability of E^* without delay and diffusion.

Turing instability occurs when there is an $n \in \mathbb{N}$ such that $A_n < 0$ or $B_n + C < 0$ [22, 27]. Obviously, $A_n > A_0 > 0$ for all $n \in \mathbb{N}$. So the condition that guaranteeing Turing instability can only be

$$B_n + C = d_1 d_2 \frac{n^4}{l^4} - (l_{22}d_1 + l_{11}d_2)\frac{n^2}{l^2} + B_0 + C < 0.$$

If $l_{22} < 0$, we can deduce that $B_n + C > 0$. In the following, we consider the case for $l_{22} > 0$. We will derive the condition for Turing instability choosing d_2 as bifurcation parameter. For convenience, denote

$$d_2(n^2) = l^2 \frac{l_{22}d_1 n^2 - (B_0 + C)l^2}{n^2(d_1 n^2 - l_{11}l^2)}.$$

Since $l_{11} < 0$, we have $d_1 n^2 - l_{11}l^2 > 0$, thus, $B_n + C < 0$ is equivalent to $d_2 < d_2(n^2)$. We need to find the critical N_T such that $d_2(n^2)$ reaches its maximum when $n = N_T$.

Lemma 3. *Assume that* (H1)–(H3) *hold.*

  (i) *If $l_{22} < 0$, then $B_n + C > 0$, and all the roots of Eq. (6) have negative real parts.*

 (ii) *If $l_{22} > 0$, there exists a positive integer $N_T \in \mathbb{N}$ such that $d_2^* \stackrel{\Delta}{=} d_2(N_T^2) = \max_{n \in \mathbb{N}} d_2(n^2)$. Equation (6) has at least one zero eigenvalue when $d_2 = d_2^*$. Moreover, if $d_2 > d_2^*$, then $B_n + C > 0$ for $n \in \mathbb{N}_0$, and all the roots of Eq. (6) have negative real parts; if $d_2 < d_2^*$, there exists at least an integer $n \in \mathbb{N}$ such that $B_n + C < 0$, and Eq. (6) has at least one eigenvalue with positive real part.*

Proof. The proof of (i) is obvious. Now we consider the case for $l_{22} > 0$. Let $q = n^2$, then $d_2(q) = l^2(l_{22}d_1 q - (B_0 + C)l^2)/(q(d_1 q - l_{11}l^2))$. Since $l_{11} < 0$, we have $d_1 q - l_{11}l^2 > 0$. We can deduce that $d_2(q) > 0$ if and only if $q > (l^2(B_0 + C))/(l_{22}d_1)$. Taking the derivative of $d_2(q)$ with respective to q yields

$$d_2'(q) = \frac{l^2}{q^2(d_1 q - l_{11}l^2)^2} \left[-l_{22}d_1^2 q^2 + 2d_1 l^2(B_0 + C)q - l_{11}(B_0 + C)l^4 \right]$$

$$\begin{cases} > 0, & 0 < q < q^*, \\ < 0, & q > q^*, \end{cases}$$

where $q^* = (l^2[B_0 + C + \sqrt{(B_0 + C)(B_0 + C - l_{11}l_{22})}])/(l_{22}d_1)$. Clearly, $d_2(q)$ reaches its maximum at $q = q^*$. Define

$$N_T = \begin{cases} \lfloor \sqrt{q^*} \rfloor & \text{if } d_2(\lfloor \sqrt{q^*} \rfloor^2) > d_2((\lfloor \sqrt{q^*} \rfloor + 1)^2), \\ \lfloor \sqrt{q^*} \rfloor + 1 & \text{if } d_2(\lfloor \sqrt{q^*} \rfloor^2) < d_2((\lfloor \sqrt{q^*} \rfloor + 1)^2), \end{cases}$$

where $\lfloor \cdot \rfloor$ is the floor function. We have $d_2(N_T^2) = \max_{n \in \mathbb{N}} d_2(n^2)$. Hence, when $d_2 > d_2(N_T^2)$, $B_n + C > 0$ for $n \in \mathbb{N}_0$. When $0 < d_2 < d_2(N_T^2)$, there exists N_1 and N_2 such that

$$B_n + C \begin{cases} \geqslant 0 & \text{for } n \leqslant N_1 \text{ or } n \geqslant N_2, \\ < 0 & \text{for } N_1 < n < N_2, \end{cases}$$

where $N_1 = \lfloor n_1 \rfloor$ and N_2 is defined by

$$N_2 = \begin{cases} n_2 & \text{if } n_2 \text{ is an integer}, \\ \lfloor n_2 \rfloor + 1 & \text{if } n_2 \text{ is not an integer} \end{cases}$$

with n_1 and n_2 being positive roots of $B_n + C = 0$, namely,

$$n_1 = l\sqrt{\frac{l_{22}}{2d_2} + \frac{l_{11}}{2d_1} + \frac{1}{2d_1 d_2}\sqrt{(l_{22}d_1 + l_{11}d_2)^2 - 4d_1 d_2(B_0 + C)}},$$
$$n_2 = l\sqrt{\frac{l_{22}}{2d_2} + \frac{l_{11}}{2d_1} - \frac{1}{2d_1 d_2}\sqrt{(l_{22}d_1 + l_{11}d_2)^2 - 4d_1 d_2(B_0 + C)}}.$$
$\square$

Theorem 1. *Suppose that* (H1)–(H3) *hold. For system* (1) *with* $\tau = 0$, *we have the following conclusions*:

   (i) *If* $l_{22} < 0$, *the positive equilibrium* E^* *is asymptotically stable*;
  (ii) *If* $l_{22} > 0$, E^* *is asymptotically stable when* $d_2 > d_2^*$, *and* E^* *is unstable when* $0 < d_2 < d_2^*$. *Moreover*, E^* *undergoes a Turing instability when* $d_2 = d_2^*$.

Fix parameters:

$$\begin{aligned} a &= 0.3, & b &= 0.5, & c &= 0.5, & d &= 0.2, & e &= 0.02, \\ \theta &= 0.26, & \mu &= 0.18, & k &= 0.15, & d_1 &= 0.1, & l &= 3. \end{aligned} \tag{7}$$
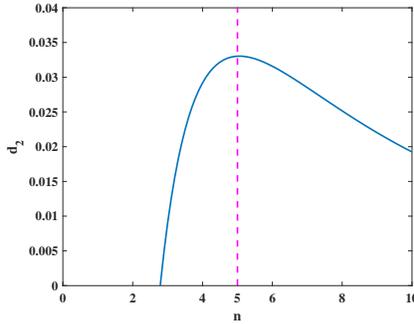
Figure 1. The diagram of $d_2(n^2)$ on the n, d_2-plane.

We can verify that (H1) and (H2) hold, and system (1) has a unique equilibrium $E^*(N^*, P^*) = (1.1061, 0.6894)$. We can also verify that (H3) holds, which means that $E^*(N^*, P^*)$ is stable for the system without diffusion and delay. In addition, we can get that $l_{22} = 0.3080 > 0$. When $n = 5.1$, $d_2(n^2)$ reaches its maximum. Thus, $N_T = 5$, $d_2^* = d_2(N_T^2) = 0.0330$.

If we decrease θ to 0 and keep the other parameters the same as in (7), system (1) has a unique equilibrium $E^*(N^*, P^*) = (d/c, (ac - de)/(bd - ck)) = (0.4, 5.84)$. It is easy to see that $l_{22} = 0$, thus $A_n > 0$ and $B_n + C > 0$ under assumption of (H1)–(H3), which means that Turing instability will not occur.

2.3 Hopf bifurcation

From Theorem 1, under assumption of (H1)–(H3), if $l_{22} < 0$ or $l_{22} > 0$ and $d_2 > d_2^*$, we can conclude that $A_n > 0$ and $B_n + C > 0$, and E^* is asymptotically stable when $\tau = 0$. Suppose that

(H4) $l_{22} < 0$;
(H5) $l_{22} > 0$ and $d_2 > d_2^*$.

In the following, taking τ as the bifurcation parameter, we seek the critical values of τ such that Eq. (5) has a pair of simple purely imaginary eigenvalues. Let $\pm i\omega_n$ ($\omega_n > 0$) be a pair of purely imaginary roots of Eq. (5), then we have

$$\omega_n^2 - B_n = C \cos \omega_n \tau, \qquad A_n \omega_n = C \sin \omega_n \tau.$$

Let $\rho_n = \omega_n^2$, we can get that

$$\rho_n^2 + T_n \rho_n + D_n = 0, \tag{8}$$

where

$$T_n = A_n^2 - 2B_n$$
$$= (d_1^2 + d_2^2)\frac{n^4}{l^4} - 2(l_{11}d_1 + l_{22}d_2)\frac{n^2}{l^2} + l_{11}^2 + l_{22}^2 + 2l_{12}l_{21},$$
$$D_n = B_n^2 - C^2 = (B_n + C)(B_n - C).$$

Since $B_n + C > 0$ and $C < 0$, $B_n - C > B_n + C > 0$, then we have $D_n > 0$. Denote $F_n = T_n^2 - 4D_n$. Since the signs of T_n and F_n are uncertain, we need to discuss in different cases, and we have the following lemma.

Lemma 4. *Suppose that* (H1)–(H3) *hold, and* (H4) *or* (H5) *holds.*

(i) *If for all $n \in \mathbb{N}_0$, $F_n < 0$ or $F_n = 0$, $T_n \geqslant 0$ or $F_n > 0$, $T_n > 0$, then* (8) *has no positive roots, and Eq.* (5) *has no purely imaginary roots.*

(ii) *If there exists $n \in \mathbb{N}_0$ such that $F_n > 0$, $T_n < 0$, then* (8) *has two positive roots $\rho_n^\pm = (-T_n \pm \sqrt{F_n})/2$, and Eq.* (5) *has two pairs of purely imaginary roots $\pm \mathrm{i}\omega_n^\pm = \pm \mathrm{i}\sqrt{\rho_n^\pm}$.*

Remark 1. In fact, when $F_n = 0$, $T_n < 0$, (8) has a positive double root, consequently, (5) has a pair of purely imaginary double roots. It may arise resonant double Hopf bifurcation. In this paper, we do not consider this case.

Denote $\mathcal{D} = \{\bar{n} \in \mathbb{N}_0 : F_n > 0, T_n < 0\}$. When (8) has two positive roots $\rho_n^\pm$, we can get that Eq. (5) has two pairs of purely imaginary roots $\pm \mathrm{i}\omega_n^\pm = \pm \mathrm{i}\sqrt{\rho_n^\pm}$. Recall that $C < 0$ and $A_n > 0$, then $\sin \omega_n \tau = A_n \omega_n / C < 0$, and we have

$$\tau_{n,j}^\pm = \frac{1}{\omega_n^\pm}\left(2\pi - \arccos \frac{\omega_n^{\pm 2} - B_n}{C} + 2j\pi\right), \quad j = 0, 1, 2 \dots . \tag{9}$$

Lemma 5. *Suppose that* (H1)–(H3) *hold, and* (H4) *or* (H5) *holds. If $F_n > 0$, then* $\operatorname{Re} \lambda'(\tau_{n,j}^+) > 0$, $\operatorname{Re} \lambda'(\tau_{n,j}^-) < 0$ *for $j \in \mathbb{N}_0$.*

Proof. Taking the derivative of both sides of Eq. (5) with respect to τ, we get

$$\left[\frac{\mathrm{d}\lambda}{\mathrm{d}\tau}\right]^{-1} = \frac{(2\lambda + A_n)\mathrm{e}^{\lambda\tau}}{C\lambda} - \frac{\tau}{\lambda}.$$

Then

$$\begin{aligned}
\operatorname{Re}\left[\frac{\mathrm{d}\lambda}{\mathrm{d}\tau}\right]^{-1}_{\tau=\tau_{n,j}^\pm} &= \operatorname{Re}\left[\frac{(2\mathrm{i}\omega_n^\pm + A_n)(\cos\omega_n^\pm\tau + \mathrm{i}\sin\omega_n^\pm\tau)}{C\mathrm{i}\omega_n^\pm}\right] \\
&= \frac{2\omega_n^\pm\cos\omega_n^\pm\tau + A_n\sin\omega_n^\pm\tau}{C\omega_n^\pm} = \frac{2(\omega_n^{\pm 2} - B_n) + A_n^2}{C^2} \\
&= \frac{\pm\sqrt{F_n}}{C^2}.
\end{aligned}$$

Therefore, $\operatorname{Re}\lambda'(\tau_{n,j}^+) > 0$, $\operatorname{Re}\lambda'(\tau_{n,j}^-) < 0$ for $F_n > 0$. $\square$

Lemma 5 tells that transversality condition holds and the Hopf bifurcation occurs at $\tau = \tau_{n,j}^\pm$ with $n \in \mathcal{D}$ and $j \in \mathbb{N}_0$. From (9) we have that $\tau_{n,0}^+ < \tau_{n,0}^-$ for all $n \in \mathcal{D}$. We can define the smallest τ so that the stability will change,

$$\tau^* = \tau_{n_0,0}^+ = \min\{\tau_{n,0}^+, n \in \mathcal{D}\}.$$

Then we have the following result.

Theorem 2. *Assume that* (H1)–(H3) *hold, and* (H4) *or* (H5) *holds.*

(i) *If $F_n < 0$ or $F_n = 0$, $T_n \geqslant 0$, or $F_n > 0$, $T_n > 0$ for all $n \in \mathbb{N}_0$, then the positive equilibrium E^* of system* (1) *is locally asymptotically stable for any $\tau \geqslant 0$.*

(ii) *If there exists $n \in \mathbb{N}_0$ such that $F_n > 0$, $T_n < 0$. System* (1) *undergoes a Hopf bifurcation at E^* when $\tau = \tau_{0,j}^+$ ($\tau = \tau_{0,j}^-$) for $j \in \mathbb{N}_0$, and the bifurcating periodic solutions are spatially homogeneous. System* (1) *undergoes a Hopf bifurcation at E^* $\tau = \tau_{n,j}^+$ ($\tau = \tau_{n,j}^-$) for $j \in \mathbb{N}_0$ and $n \in \mathcal{D}$, and the bifurcating periodic solutions are spatially inhomogeneous.*

(iii) *If there exists $n \in \mathbb{N}_0$ such that $F_n > 0$, $T_n < 0$, then E^* of system* (1) *is locally asymptotically stable when $0 \leqslant \tau < \tau^*$, and E^* is unstable for $\tau \in (\tau^*, \tau^* + \epsilon)$ with some $\epsilon > 0$.*

Proof. (i) Let (H1)–(H3) hold, and (H4) or (H5) holds. From Lemma 3 all the roots of Eq. (5) have negative real parts when $\tau = 0$. From Corollary 2.4 in [21] the sum of the multiplicities of the roots of Eq. (5) in the open right half-plane changes only if a root appears on or crosses the imaginary axis. Recalling that $B_n + C > 0$, it is easy to see that $\lambda = 0$ is not the root of Eq. (5). From Lemma 4(i) Eq. (5) has no purely imaginary roots under the assumption. Therefore, the sum of the multiplicities of the roots of Eq. (5) in the open right half-plane does not change, and all the roots of Eq. (5) have negative real parts, thus the positive equilibrium E^* of system (1) is locally asymptotically stable for any $\tau \geqslant 0$.

(ii) From Lemma 4 Eq. (5) has a pair of purely imaginary roots $\pm i\omega_n^+$ ($\pm i\omega_n^-$) when $\tau = \tau_{n,j}^+$ ($\tau = \tau_{n,j}^-$) for $n \in \mathcal{D}$ and $j \in \mathbb{N}_0$. Hence, from the transversality condition in Lemma 5 and Corollary 2.4 in [21] we can obtain the conclusion.

(iii) From the previous discussion τ^* is the smallest τ so that the stability will change, and $\operatorname{Re} \lambda'(\tau_{n,0}^+) > 0$, thus we can obtain the conclusion. $\qquad\square$

Remark 2. From Lemma 5 we have $\operatorname{Re} \lambda'(\tau_{n,j}^+) > 0$, $\operatorname{Re} \lambda'(\tau_{n,j}^-) < 0$ for $j \in \mathbb{N}_0$, thus stability switch may occur. If the order for the critical values of Hopf bifurcation for delay can be verified, then the stable intervals and unstable intervals of τ can be obtained. However, for system (1), it is not easy to verify the order of $\tau_{n,j}^\pm$, therefore, the stable intervals and unstable intervals of τ for E^* cannot be obtained.

Combining Theorems 1 and 2, we have the following results.

Theorem 3. *Assume that* (H1)–(H3) *hold, $l_{22} > 0$ and $F_0 > 0$, $T_0 < 0$.*

(i) *If $d_2 > d_2^*$ and $0 \leqslant \tau < \tau^*$, E^* is asymptotically stable. If $d_2 > d_2^*$ and $\tau \in (\tau^*, \tau^* + \epsilon)$ with some $\epsilon > 0$, E^* is unstable.*

(ii) *Assume that $\tau^* = \tau_{0,0}^+$. E^* is unstable for $0 < d_2 < d_2^*$ and $\tau \in [0, \tau^* + \epsilon)$.*

Proof. (i) From Theorem 2(iii), if (H5) holds, then E^* of system (1) is locally asymptotically stable when $0 \leqslant \tau < \tau^*$, and E^* is unstable for $\tau \in (0, \tau^* + \epsilon)$ with some $\epsilon > 0$.

(ii) From Lemma 3(ii) Eq. (5) has at least one eigenvalue with positive real part if $0 < d_2 < d_2^*$ when $\tau = 0$. Since (H3) holds, we have $B_0 + C > 0$. Combining with $C < 0$, we have $B_0 - C > B_0 + C > 0$, then we get $D_0 > 0$. If $F_0 > 0$, $T_0 < 0$, Eq. (5) has a pair of purely imaginary roots $\pm i\omega_0^+$ ($\pm i\omega_0^-$) when $\tau = \tau_{0,0}^+$ ($\tau_{0,0}^-$). It is easy to verify that $\tau = \tau_{0,0}^+ < \tau_{0,0}^-$. Similar as Lemma 5, we can get $\operatorname{Re}\lambda'(\tau_{0,0}^+) > 0$. If $\tau^* = \tau_{0,0}^+$, from Corollary 2.4 in [21] Eq. (5) has at least one eigenvalue with positive real part when $0 < d_2 < d_2^*$ and $\tau \in (0, \tau^*]$, and it has at least three eigenvalues with positive real parts when $0 < d_2 < d_2^*$ and $\tau \in (\tau^*, \tau^* + \epsilon)$. This completes the proof. $\qquad\square$

Remark 3. Suppose that (H1)–(H3) hold, and $l_{22} > 0$. If $\tau = \tau^*$ and $d_2 = d_2^*$, then the characteristic equation (5) has a pair of purely imaginary roots $\pm i\omega_n$ and a simple zero eigenvalue for $n = N_T$, all other eigenvalues have strictly negative real parts. System (1) undergoes a Turing–Hopf bifurcation at E^* when $(\tau, d_2) = (\tau^*, d_2^*)$.

3   Normal form of Turing–Hopf bifurcation

In this section, we shall study the spatiotemporal dynamics of system (1) by using the center manifold reduction and normal form theory. The amplitude equations are finally obtained to describe dynamics near the critical Turing–Hopf singularity.

Define the real-valued Sobolev space

$$X := \left\{ (u, v)^{\mathrm{T}} \colon u, v \in H^2(0, l\pi),\ \frac{\partial u}{\partial x}(0, t) = \frac{\partial v}{\partial x}(l\pi, t) = 0 \right\}$$

and the corresponding complexification space $X_{\mathbb{C}} := X \oplus iX = \{U_1 + iU_2,\ U_1, U_2 \in X\}$ with the general complex-valued L^2 inner product $\langle U_1, U_2 \rangle = \int_0^{l\pi} (\bar{u}_1 u_2 + \bar{v}_1 v_2)\,\mathrm{d}x$ for $U_1 = (u_1, v_1)^{\mathrm{T}}$, $U_2 = (u_2, v_2)^{\mathrm{T}} \in X_{\mathbb{C}}$. Let $C := C([-1, 0], X_{\mathbb{C}})$ denotes the phase space with the supremum norm. We write $U(t) = (u(x, t), v(x, t))^{\mathrm{T}}$ and $U_t \in C$ for $U_t(\theta) = U(t + \theta)$, $-1 \leqslant \theta \leqslant 0$.

Let $\hat{u}(x, t) = N(x, \tau t) - N^*$, $\hat{v}(x, t) = P(x, \tau t) - P^*$, and drop the hats for simplicity of notation, then system (1) can be transformed to

$$\begin{aligned}
\frac{\partial u}{\partial t} &= \tau \big[d_1 \Delta u - (bP^* + e)u - bN^* v + kv(t-1) + f_1(u_t, v_t) \big], \\
\frac{\partial v}{\partial t} &= \tau \left[d_2 \Delta v + cP^* u + \frac{\theta P^*(P^{*2} - \mu^2)}{(\mu^2 + P^{*2})^2} v + f_2(u_t, v_t) \right],
\end{aligned} \tag{10}$$

where for $\phi_1, \phi_2 \in C := C([-1, 0], X_{\mathbb{C}})$,

$$\begin{aligned}
f_1(\phi_1, \phi_2) &= -b\phi_1(0)\phi_2(0), \\
f_2(\phi_1, \phi_2) &= c\phi_1(0)\phi_2(0) - \frac{\theta\mu^2(\mu^2 - 3P^{*2})}{(\mu^2 + P^{*2})^3} \phi_2^2(0) \\
&\quad + \frac{4\theta P^* \mu^2(\mu^2 - P^{*2})}{(\mu^2 + P^{*2})^4} \phi_2^3(0).
\end{aligned} \tag{11}$$

In order to study the dynamics near the Turing–Hopf bifurcation point, we introduce

$$BC := \Big\{ \psi : [-1,0] \to X_\mathbb{C} \ \Big| \ \psi \text{ is continuous on } [-1,0),$$

$$\text{and there exists } \lim_{\theta \to 0^-} \psi(\theta) \in X_\mathbb{C} \Big\}.$$

Denote $m = (\tau, d_2)$, $m^* = (\tau^*, d_2^*)$, $m_\varepsilon = (\tau_\varepsilon, d_{2\varepsilon})$, and $m = m^* + m_\varepsilon$. Then system (10) undergoes a Turing–Hopf bifurcation at the equilibrium $(0,0)$ when $m_\varepsilon = (0,0)$, and we can rewrite system (10) in the space BC as

$$\frac{\mathrm{dU(t)}}{\mathrm{dt}} = AU_t + X_0 \mathscr{F}(m_\varepsilon, U_t), \tag{12}$$

where

$$X_0(\theta) = \begin{cases} 0, & \theta \in [-1,0), \\ I, & \theta = 0, \end{cases}$$

and A is an operator from $C_0^1 := \{\varphi \in C \colon \dot\varphi \in C, \ \varphi(0) \in \mathrm{dom}(\Delta)\}$ to BC defined by

$$A\varphi = \dot\varphi + X_0 \big[\tau^* D_0 \Delta \varphi(0) + \tau^* L_0(\varphi) - \dot\varphi(0) \big].$$

Here $D_0 = D(m^*) = \mathrm{diag}(d_1, d_2^*)$, $L_0 : C \to X_\mathbb{C}$ is a linear operator given by $L_0(\varphi) = L(m^*)(\varphi)$ with

$$L(m)(\varphi) = L_1'\varphi(0) + L_2\varphi(-1)$$

with L_1' and L_2 defined in (4), and $\mathscr{F} : \mathbb{R}^2 \times C \to X_\mathbb{C}$ is a nonlinear operator defined by

$$\mathscr{F}(m_\varepsilon, \phi) = \big[d_{2\varepsilon}\tau^* \, \mathrm{diag}\{0,1\} + \tau_\varepsilon D_0 \big] \Delta\varphi(0)$$
$$+ \tau_\varepsilon L(m)(\varphi) + (\tau^* + \tau_\varepsilon) F(m_\varepsilon, \varphi)$$

with

$$F(m_\varepsilon, \varphi) = (\tau^* + \tau_\varepsilon)\big(f_1(\varphi_1, \varphi_2), f_2(\varphi_1, \varphi_2)\big)^{\mathrm{T}},$$

where f_1 and f_2 are defined in (11).

Let $C^* := C([0,1], X_\mathbb{C})$ be the conjugate space of C. Define $(\cdot, \cdot)_k$ as the adjoint bilinear form on $C^* \times C$:

$$(\alpha, \beta)_k = \alpha(0)\beta(0) - \int_{-1}^{0} \int_{\xi=0}^{\theta} \alpha(\xi - \theta) \, \mathrm{d}\eta_k(0,\theta)\beta(\xi) \, \mathrm{d}\xi, \quad \mathrm{k} = 1,2,$$

and $\eta_k \in BV([-1,0], \mathbb{C}^{2\times 2})$ are given by

$$-\frac{n_k^2}{l^2} D_0\varphi(0) + L_0(\varphi) = \int_{-1}^{0} \mathrm{d}\eta_\mathrm{k}(0,\theta)\varphi(\theta), \quad \varphi \in \mathrm{C}, \ \mathrm{k} = 1,2.$$

Denote A^* as the adjoint operator of A on $C^* := C([0,1], X_{\mathbb{C}})$, and let $\{\phi_1(\theta)b_{n_1}, \phi_2(\theta)b_{n_2}\}$ and $\{\psi_1(s)b_{n_1}, \psi_2(s)b_{n_2}\}$ be the eigenfunctions of A and A^* relative to $\Lambda = \{i\omega_0\tau^*, 0\}$ such that $\phi_1, \phi_2 \in C$, $\psi_1, \psi_2 \in C^*$, and

$$(\psi_1, \phi_1)_1 = 1, \qquad (\psi_1, \bar{\phi}_1)_1 = 0, \qquad (\psi_2, \phi_2)_2 = 1.$$

By a straightforward calculation we have

$$\phi_1(\theta) = q(0)\mathrm{e}^{i\omega_0\tau^*\theta}, \qquad \psi_1(s) = M_1 q^*(0)\mathrm{e}^{-i\omega_0\tau^*s},$$
$$\phi_2(\theta) = p(0), \qquad \psi_2(s) = M_2 p^*(0),$$

where $q(0) = (1, q_1)^{\mathrm{T}}$, $q^*(0) = (1, q_2)$, $p(0) = (1, p_1)^{\mathrm{T}}$, $p^*(0) = (1, p_2)$, and

$$q_1 = \frac{l_{21}}{i\omega_0 - l_{22}}, \qquad q_2 = \frac{i\omega_0 - l_{11}}{l_{21}}, \qquad p_1 = \frac{d_1\frac{n_2^2}{l^2} - l_{11}}{l_{12} + k}, \qquad p_2 = \frac{d_1\frac{n_2^2}{l^2} - l_{11}}{l_{21}},$$
$$M_1 = \frac{1}{1 + q_1 q_2 + q_1 k\tau^*\mathrm{e}^{-i\omega_0\tau^*}}, \qquad M_2 = \frac{1}{1 + p_1 p_2 + p_1 k\tau^*}.$$

Denote $\Phi_1 = (\phi_1, \bar{\phi}_1)$, $\Psi_1 = (\psi_1^{\mathrm{T}}, \bar{\psi}_1^{\mathrm{T}})^{\mathrm{T}}$, and $\Phi_2 = \phi_2$, $\Psi_2 = \psi_2$. From the discussion above the phase space BC can be decomposed as

$$BC = P \oplus \mathrm{Ker}\,\pi,$$

where P is center subspace spanned by the basis eigenfunctions of the linear operator A associated with the eigenvalues $\{\pm i\omega_0\tau^*, 0\}$, and $\mathrm{Ker}\,\pi$ is the complementary space of P with $\pi : BC \to P$ being the projection defined by

$$\pi\varphi = \sum_{k=1}^{2} \Phi_k \big(\Psi_k, \langle \varphi(\cdot), b_{n_k} \rangle\big)_k b_{n_k},$$

where $\varphi_{n_k}^{(1)} = (b_{n_k}, 0)^{\mathrm{T}}$, $\varphi_{n_k}^{(2)} = (0, b_{n_k})^{\mathrm{T}}$, and $\langle \cdot, b_{n_k} \rangle = \langle \cdot, \varphi_{n_k}^{(1)} + \varphi_{n_k}^{(2)} \rangle$.

Then $U_t \in C_0^1$ can be decomposed as

$$U_t(\theta) = \sum_{k=1}^{2} \Phi_k(\theta)\big(\Psi_k, \langle U_t, b_{n_k} \rangle\big)_k b_{n_k} + y(\theta) = \sum_{k=1}^{2} \Phi_k(\theta)\tilde{z}_k(t)b_{n_k} + y(\theta)$$

with $\tilde{z}_1 = (z_1, \bar{z}_1)$, $\tilde{z}_2 = z_2$, and $y \in Q^1 := C_0^1 \cap \mathrm{Ker}\,\pi$. Then system (12) on BC is equivalent to the following system:

$$\dot{z} = Bz + \Psi(0) \begin{pmatrix} \langle \mathscr{F}(m_\varepsilon, \sum_{k=1}^{2} \Phi_k \tilde{z}_k(t)b_{n_k} + y), b_{n_1} \rangle \\ \langle \mathscr{F}(m_\varepsilon, \sum_{k=1}^{2} \Phi_k \tilde{z}_k(t)b_{n_k} + y), b_{n_2} \rangle \end{pmatrix},$$

$$\frac{\mathrm{d}}{\mathrm{d}t} y = A_{Q^1} y - (I - \pi)X_0 \mathscr{F}\bigg(m_\varepsilon, \sum_{k=1}^{2} \Phi_k \tilde{z}_k(t)b_{n_k} + y\bigg),$$

where $z = (z_1, \bar{z}_1, z_2)$, $B = \operatorname{diag}(\mathrm{i}\omega_0\tau^*, -\mathrm{i}\omega_0\tau^*, 0)$, $\Psi = \operatorname{diag}(\Phi_1, \Phi_2)$, and A_{Q^1} is the restriction of A as an operator from Q^1 to $\operatorname{Ker}\pi$.

From Theorem 3.2 in [1, 26] the normal forms of system (1) up to third order near a Turing–Hopf singularity $m = m^*$ are obtained:

$$
\begin{aligned}
\dot{z}_1 &= \mathrm{i}\omega_0\tau^* z_1 + \frac{1}{2}\mathrm{f}_{11}^{11}\alpha_1 z_1 + \frac{1}{2}\mathrm{f}_{21}^{11}\alpha_2 z_1 + \frac{1}{6}\mathrm{g}_{210}^{11}z_1^2\bar{z}_1 + \frac{1}{6}\mathrm{g}_{102}^{11}z_1 z_2^2 + \text{h.o.t.},\\
\dot{\bar{z}}_1 &= -\mathrm{i}\omega_0\tau^* z_1 + \frac{1}{2}\mathrm{f}_{11}^{12}\alpha_1 \bar{z}_1 + \frac{1}{2}\mathrm{f}_{21}^{12}\alpha_2 \bar{z}_1 + \frac{1}{6}\mathrm{g}_{210}^{12}\bar{z}_1^2 z_1 + \frac{1}{6}\mathrm{g}_{102}^{12}\bar{z}_1 z_2^2 + \text{h.o.t.}, \quad (13)\\
\dot{z}_2 &= \frac{1}{2}f_{12}^{13}\alpha_1 z_2 + \frac{1}{2}f_{22}^{13}\alpha_2 z_2 + \frac{1}{6}g_{111}^{13}z_1\bar{z}_1 z_2 + \frac{1}{6}g_{003}^{13}z_2^3 + \text{h.o.t.}
\end{aligned}
$$

with $(\alpha_1, \alpha_2) = (\tau_\varepsilon, d_{2\varepsilon})$, $f_{mn}^{12} = \bar{f}_{mn}^{11}$, $g_{mnk}^{12} = \bar{g}_{mnk}^{11}$, and

$$
\begin{aligned}
f_{11}^{11} &= 2\psi_1(0)\big[L_1'\phi_1(0) + L_2\phi_1(-1)\big], \qquad f_{21}^{11} = 0,\\
f_{12}^{13} &= 2\psi_2(0)\bigg[-\frac{n_2^2}{l^2}D_0\phi_2(0) + L_1'\phi_2(0) + L_2\phi_2(-1)\bigg],\\
f_{22}^{13} &= 2\psi_2(0)\bigg[-\frac{n_2^2}{l^2}\tau^*\operatorname{diag}\{0,1\}\phi_2(0)\bigg],\\
g_{210}^{11} &= f_{210}^{11} + \frac{3}{2\mathrm{i}\omega_0\tau^*}\bigg(-f_{110}^{11}f_{200}^{11} + f_{110}^{11}f_{110}^{12} + \frac{2}{3}f_{020}^{11}f_{200}^{12}\bigg)\\
&\quad + \frac{3}{2}\psi_1(0)\big[S_{yz_1}\big(\langle h_{110}(\theta)b_{n_1}, b_{n_1}\rangle\big) + S_{y\bar{z}_1}\big(\langle h_{200}(\theta)b_{n_1}, b_{n_1}\rangle\big)\big],\\
g_{102}^{11} &= f_{102}^{11} + \frac{3}{2\mathrm{i}\omega_0\tau^*}\big(-2f_{002}^{11}f_{200}^{11} + f_{002}^{12}f_{110}^{11} + 2f_{002}^{11}f_{101}^{13}\big)\\
&\quad + \frac{3}{2}\psi_1(0)\big[S_{yz_1}\big(\langle h_{002}(\theta)b_{n_1}, b_{n_1}\rangle\big) + S_{yz_2}\big(\langle h_{101}(\theta)b_{n_2}, b_{n_1}\rangle\big)\big],\\
g_{111}^{13} &= f_{111}^{13} + \frac{3}{2\mathrm{i}\omega_0\tau^*}\big(-f_{101}^{13}f_{110}^{11} + f_{011}^{13}f_{110}^{12}\big) + \frac{3}{2}\psi_2(0)\big[S_{yz_1}\big(\langle h_{011}(\theta)b_{n_1}, b_{n_2}\rangle\big)\\
&\quad + S_{y\bar{z}_1}\big(\langle h_{101}(\theta)b_{n_1}, b_{n_2}\rangle\big) + S_{yz_2}\big(\langle h_{110}(\theta)b_{n_2}, b_{n_2}\rangle\big)\big],\\
g_{003}^{13} &= f_{003}^{13} + \frac{3}{2\mathrm{i}\omega_0\tau^*}\big(-f_{002}^{11}f_{101}^{13} + f_{002}^{12}f_{011}^{13}\big) + \frac{3}{2}\psi_2(0)\big[S_{yz_2}\big(\langle h_{002}(\theta)b_{n_2}, b_{n_2}\rangle\big)\big],
\end{aligned}
$$

where $f_{mnk}^{12} = \bar{f}_{mnk}^{11}$ and

$$
\begin{aligned}
f_{mnk}^{11} &= \frac{1}{\sqrt{l\pi}}\psi_1(0)F_{mnk}, \quad f_{mnk}^{13} = \frac{1}{\sqrt{l\pi}}\psi_2(0)F_{mnk} \quad \text{when } m+n+k = 2,\\
f_{mnk}^{11} &= \frac{1}{l\pi}\psi_1(0)F_{mnk}, \qquad f_{mnk}^{13} = \frac{1}{l\pi}\psi_2(0)F_{mnk} \qquad \text{when } m+n+k = 3,
\end{aligned}
$$

$$
\begin{aligned}
\langle h_{200}(\theta)b_{n_1}, b_{n_1}\rangle &= \frac{\mathrm{e}^{2\mathrm{i}\omega_0\tau^*\theta}}{l\pi}\big[2\mathrm{i}\omega_0\tau^* - \tau^* \mathrm{L}_0\big(\mathrm{e}^{2\mathrm{i}\omega_0\tau^*} \cdot \mathrm{I}_\mathrm{d}\big)\big]^{-1}\mathrm{F}_{200}\\
&\quad - \frac{1}{\mathrm{i}\omega_0\tau^*\sqrt{l\pi}}\bigg[f_{200}^{11}\phi_1(\theta) + \frac{1}{3}f_{200}^{12}\bar{\phi}_1(\theta)\bigg],
\end{aligned}
$$

$$\langle h_{110}(\theta)b_{n_1}, b_{n_1}\rangle = -\frac{1}{l\pi}\big[\tau^* L_0(I_d)\big]^{-1}F_{110} + \frac{1}{i\omega_0\tau^*\sqrt{l\pi}}\big[f_{110}^{11}\phi_1(\theta) - f_{110}^{12}\bar{\phi}_1(\theta)\big],$$

$$\langle h_{110}(\theta)b_{n_2}, b_{n_2}\rangle = \langle h_{110}(\theta)b_{n_1}, b_{n_1}\rangle,$$

$$\langle h_{101}(\theta)b_{n_2}, b_{n_1}\rangle = \frac{e^{i\omega_0\tau^*\theta}}{l\pi}\Big[i\omega_0\tau^* + \frac{n_2^2}{l^2}\tau^* D_0 - \tau^* L_0\big(e^{i\omega_0\tau^*}\cdot I_d\big)\Big]^{-1}F_{101}$$

$$\qquad - \frac{1}{i\omega_0\tau^*\sqrt{l\pi}}f_{101}^{13}\phi_2(0),$$

$$\langle h_{011}(\theta)b_{n_1}, b_{n_2}\rangle = \frac{e^{-i\omega_0\tau^*\theta}}{l\pi}\Big[-i\omega_0\tau^* + \frac{n_2^2}{l^2}\tau^* D_0 - \tau^* L_0\big(e^{-i\omega_0\tau^*}\cdot I_d\big)\Big]^{-1}F_{011}$$

$$\qquad + \frac{1}{i\omega_0\tau^*\sqrt{l\pi}}f_{011}^{13}\phi_2(0),$$

$$\langle h_{002}(\theta)b_{n_1}, b_{n_1}\rangle = -\frac{1}{l\pi}\big[\tau^* L_0(I_d)\big]^{-1}F_{002} + \frac{1}{i\omega_0\tau^*\sqrt{l\pi}}\big[f_{002}^{11}\phi_1(\theta) - f_{002}^{12}\bar{\phi}_1(\theta)\big],$$

$$\langle h_{002}(\theta)b_{n_2}, b_{n_2}\rangle = \frac{1}{2l\pi}\Big[\frac{(2n_2)^2}{l^2}\tau^* D_0 - \tau^* L_0(I_d)\Big]^{-1}F_{002} + \langle h_{002}(\theta)b_{n_1}, b_{n_1}\rangle,$$

and S_{yz_i} $(i = 1, 2)$, $S_{y\bar{z}_1}$ are linear operators from Q_1 to $X_{\mathbb{C}}$ given by

$$S_{yz_i}(\varphi) = (F_{y_1(0)z_i}, F_{y_2(0)z_i})\varphi(0) + (F_{y_1(-1)z_i}, F_{y_2(-1)z_i})\varphi(-1),$$

$$S_{y\bar{z}_1}(\varphi) = (\overline{F_{y_1(0)z_1}}, \overline{F_{y_2(0)z_1}})\varphi(0) + (\overline{F_{y_1(-1)z_1}}, \overline{F_{y_2(-1)z_1}})\varphi(-1).$$

We leave the specific expressions of formulas $F_{y_i(\cdot)z_j}$ and F_{mnk} in Appendix.

Through the cylindrical coordinate transformation

$$z_1 = \tilde{\rho}e^{i\sigma}, \qquad \bar{z}_1 = \tilde{\rho}e^{-i\sigma}, \qquad z_2 = \tilde{\eta}$$

and variable substitution

$$\rho = \sqrt{\frac{|\operatorname{Re}(g_{210}^{11})|}{6}}\,\tilde{\rho}, \qquad \eta = \sqrt{\frac{|g_{003}^{13}|}{6}}\,\tilde{\eta}, \qquad \varepsilon = \operatorname{Sign}\big(\operatorname{Re}(g_{210}^{11})\big), \qquad \tilde{t} = \frac{t}{\varepsilon},$$

Eq. (13) can be written as

$$\begin{aligned} \frac{d\rho}{d\tilde{t}} &= \rho\big(\varepsilon_1(m_\varepsilon) + \rho^2 + b_0\eta^2\big), \\ \frac{d\eta}{d\tilde{t}} &= \eta\big(\varepsilon_2(m_\varepsilon) + c_0\rho^2 + \hat{d}\eta^2\big), \end{aligned} \tag{14}$$

where

$$\varepsilon_1(m_\varepsilon) = \frac{\varepsilon}{2}\big[\operatorname{Re}\big(f_{11}^{11}\big)\tau_\varepsilon + \operatorname{Re}\big(f_{21}^{11}\big)d_{2\varepsilon}\big], \qquad \varepsilon_2(m_\varepsilon) = \frac{\varepsilon}{2}\big[f_{12}^{13}\tau_\varepsilon + f_{22}^{13}d_{2\varepsilon}\big],$$

$$b_0 = \frac{\varepsilon\operatorname{Re}(g_{102}^{11})}{|g_{003}^{13}|}, \qquad c_0 = \frac{\varepsilon g_{111}^{13}}{|\operatorname{Re}(g_{210}^{11})|}, \qquad \hat{d} = \frac{\varepsilon g_{003}^{13}}{|g_{003}^{13}|} = \pm 1.$$

From [12] there are 12 distinct types of unfoldings according to the signs of coefficients b_0, c_0, $\hat{d}$, and $\hat{d} - b_0 c_0$.

4 Numerical simulations

In this section, we carry out some simulations to illustrate the results. Fix parameters:

$$a = 0.3, \qquad b = 0.5, \qquad c = 0.5, \qquad d = 0.2, \qquad e = 0.02,$$
$$\theta = 0.26, \qquad \mu = 0.18, \qquad d_1 = 0.1, \qquad l = 3. \tag{15}$$

4.1 Hopf bifurcation

In this section, we consider the effect of delay on the dynamics of system (1). Fix $d_2 = 0.04$.

It turns out that the strength of k plays an important role in the occurrence of Hopf bifurcation. Choose $k = 0.19$ such that the value of k is high. We can verify that $l_{22} > 0$, and (H1)–(H3) hold. We can get that $d_2 > d_2^* = d_2(9^2) = 0.003$, which means that (H4) holds. Moreover, we have $F_n > 0$, $T_n > 0$. From Theorem 2 E^* is asymptotically stable for $\tau > 0$, and Hopf bifurcation does not occur. When the value is decreased to $k = 0.15$, similarly, we can verify $l_{22} > 0$, and (H1)–(H3) hold. We can get that $d_2 > d_2^* = d_2(5^2) = 0.033$, which means that (H4) holds. Furthermore, $F_n > 0$, $T_n < 0$ for $n = 0, 1, 2$. According to Lemma 4, we know that Eq. (5) has two pairs of purely imaginary roots $\pm i\omega_n^\pm$ at $\tau_{n,j}^\pm$ and $\operatorname{Re} \lambda'(\tau_{n,j}^+) > 0$, $\operatorname{Re} \lambda'(\tau_{n,j}^-) < 0$. Through calculation, we can get

$$\tau_{0,0}^+ < \tau_{1,0}^+ < \tau_{2,0}^+ < \tau_{0,1}^+ < \tau_{2,0}^- < \tau_{1,1}^+ < \tau_{2,1}^+ < \tau_{1,0}^-$$
$$< \tau_{0,0}^- < \tau_{0,2}^+ < \tau_{1,2}^+ < \tau_{2,2}^+ < \tau_{2,1}^- < \cdots.$$

Thus, $\tau^* = \min\{\tau_{n,j}^\pm\} = \tau_{0,0}^+ = 9.9788$. From Theorem 3 positive equilibrium $E^*(1.1061, 0.6894)$ is locally asymptotically stable when $\tau \in [0, \tau_{0,0}^+)$ (see Fig. 2), and the bifurcating periodic solutions exist for $\tau > \tau_{0,0}^+$ (see Fig. 3).

If we decrease θ to 0 and keep the other parameters the same as in (15), we can verify that $F_n > 0$ and $T_n > 0$ when $k = 0.19$ or $k = 0.15$, which means that all the roots of Eq. (5) have negative parts, and Hopf bifurcation will not occur.
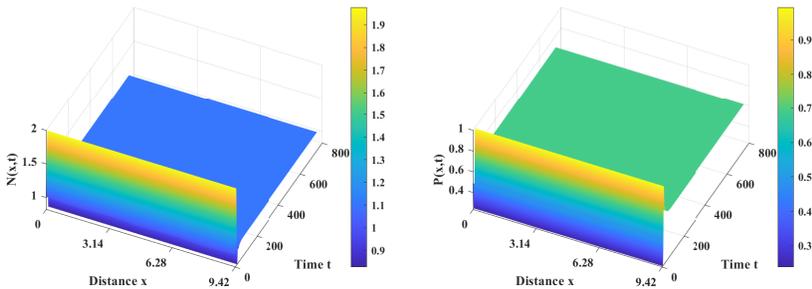

Figure 2. Numerical simulations of system (1) for (15) and $\tau = 5 < \tau^* = 9.9788$. The positive equilibrium $E^*(1.1061, 0.6894)$ of (1) is locally asymptotically stable with the initial condition $N_0(x, t) = 1 - 0.01 \cos(2x)$ and $P_0(x, t) = 0.5 + 0.01 \cos(2x)$.
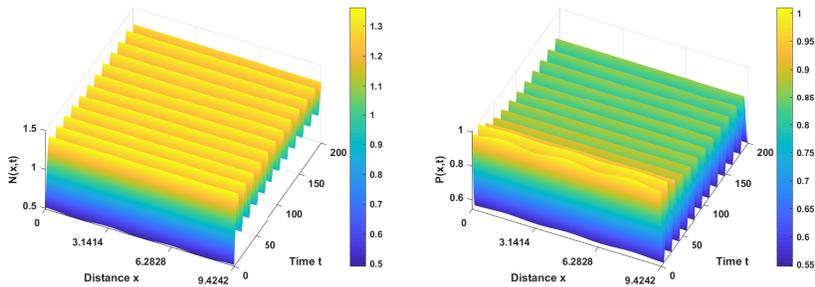
Figure 3. When $\tau = 10 > \tau^*$, the positive equilibrium $E^*(1.1061, 0.6894)$ of (1) is unstable, and there are bifurcating periodic solutions, where the initial condition $N_0(x, t) = 1 - 0.01\cos(2x)$ and $P_0(x, t) = 0.5 + 0.01\cos(2x)$.

4.2 Complex dynamics near Turing–Hopf bifurcation

In the following, we demonstrate complex phenomena of system (1) near Turing–Hopf bifurcation point. Fix the parameters as in (15) and $k = 0.15$, choose d_2 and τ as bifurcation parameters. We can draw Turing bifurcation curves and Hopf curves on d_2, τ-plane (see Fig. 4). The dashed lines are Turing bifurcation curves with $n = 3, 4, 5$ from left to right, while the solid lines are Hopf bifurcation curves $\tau_{n,0}^+$ with $n = 0, 1, 2$ from bottom to top, respectively, and the dot marked with $*$ is the Turing–Hopf intersection $(d_2^*, \tau^*) \approx (0.0330, 9.9788)$, where $d_2^* = d_2(5^2)$, $\tau^* = \tau_{0,0}^+$. From Theorem 3, when $d_2 > d_2^*$ and $\tau < \tau^*$ (the pocket of dark blue), E^* is stable. According to the normal form procedure with $n_2 = 5$, the key parameters are obtained.

$$\varepsilon_1 = -0.12322\tau_\varepsilon, \qquad \varepsilon_2 \approx 18.90161d_{2\varepsilon}, \qquad \varepsilon = -1,$$
$$\hat{d} = 1, \qquad b_0 = 2.764626, \qquad c_0 = -0.015448, \qquad \hat{d} - b_0 c_0 = 1.042708.$$

System (14) can be written as

$$\begin{aligned}
\dot{\rho} &= -\rho\left(-0.12322\tau_\varepsilon + \rho^2 + 2.764626\eta^2\right), \\
\dot{\eta} &= -\eta\left(18.90161d_{2\varepsilon} - 0.015448\rho^2 + \eta^2\right).
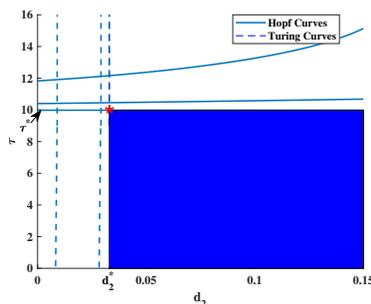\end{aligned} \qquad (16)$$

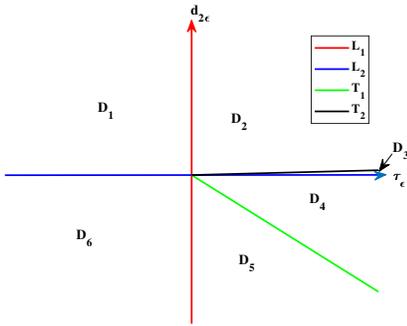**Figure 4.** The stable region and bifurcation curves in d_2, τ-plane.

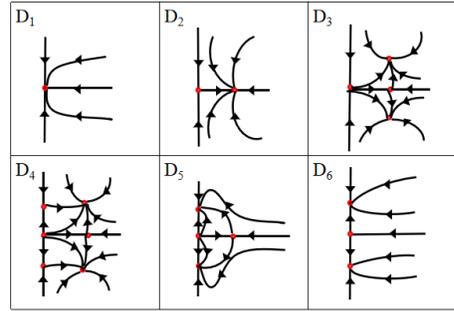**Figure 5.** The bifurcation set on the $\tau_\varepsilon, d_{2\varepsilon}$-plane.

Figure 6. The dynamical classifications in regions D_1–D_6.

Note that $\rho > 0$ and η is an arbitrary real number. By some simple calculations we find that system (16) admits the following equilibria:

$$A_0 = (0,0), \qquad A_1 = (\sqrt{0.12322\tau_\varepsilon}, 0) \quad \text{for } \tau_\varepsilon > 0,$$
$$A_2^\pm = (0, \pm\sqrt{-18.90161d_{2\varepsilon}}) \quad \text{for } d_{2\varepsilon} < 0,$$
$$A_3^\pm = (\sqrt{50.1155d_{2\varepsilon} + 0.11817\tau_\varepsilon}, \pm\sqrt{0.001826\tau_\varepsilon - 18.1274d_{2\varepsilon}})$$
$$\text{for } 50.1155d_{2\varepsilon} + 0.11817\tau_\varepsilon > 0 \text{ and } 0.001826\tau_\varepsilon - 18.1274d_{2\varepsilon} > 0.$$

Moreover, the critical bifurcation lines for system (16) are

$$L_1\text{:} \quad \tau_\varepsilon = 0; \qquad T_1\text{:} \ d_{2\varepsilon} = -0.00236\tau_\varepsilon \quad (\tau_\varepsilon > 0);$$
$$L_2\text{:} \ d_{2\varepsilon} = 0; \qquad T_2\text{:} \ d_{2\varepsilon} = 0.00010\tau_\varepsilon \quad (\tau_\varepsilon > 0).$$

From [12, Sect. 7.5] boundary equilibria A_1 and $A_2^\pm$ of (16) are bifurcated from the origin A_0 on the critical lines L_1 and L_2 through pitchfork bifurcation, respectively. The pair of equilibria $A_3^\pm$ are bifurcated from the boundary equilibria A_1 and $A_2^\pm$ on the critical lines T_2 and T_1 through pitchfork bifurcation, respectively.

Notice that the zero equilibrium A_0 of (16) corresponds to the positive equilibrium E^* of the original system (1). A_1 of (16) corresponds to the spatially homogeneous periodic solution of the original system (1). The equilibria $A_2^\pm$ in (16) correspond to the nonconstant steady state solutions of the original system (1). $A_3^\pm$ corresponds to spatially inhomogeneous periodic solutions.

The four straight lines divide the $\tau_\varepsilon, d_{2\varepsilon}$-plane into six regions denoted by D_1–D_6 (see Fig. 5) with the corresponding phase portraits shown in Fig. 6.

In region D_1, system (16) has only one equilibrium A_0, which is stable. It means that the positive equilibrium $E^*(N^*, P^*)$ of system (1) is asymptotically stable (see Fig. 7).

When the parameters pass through the line L_1 from D_1 to D_2, A_1 is bifurcated from A_0 on the pitchfork bifurcation line L_1. In region D_2, system (16) has two equilibria A_0 and A_1. A_0 is unstable, and A_1 is stable. It means that the positive equilibrium $E^*(N^*, P^*)$ of system (1) is unstable, and the spatially homogeneous periodic solution is stable (see Fig. 8).
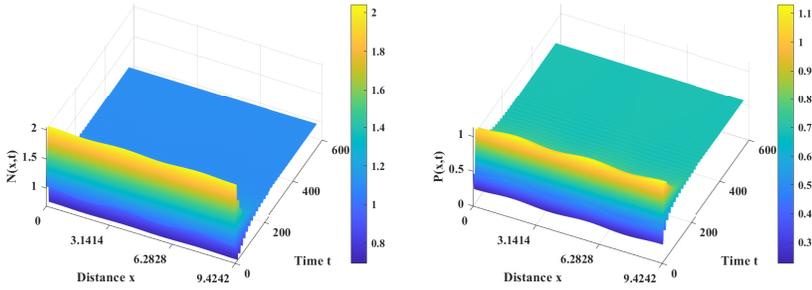
Figure 7. E^* is locally asymptotically stable for $(\tau_\varepsilon, d_{2\varepsilon}) = (-0.9788, 0.027) \in D_1$.
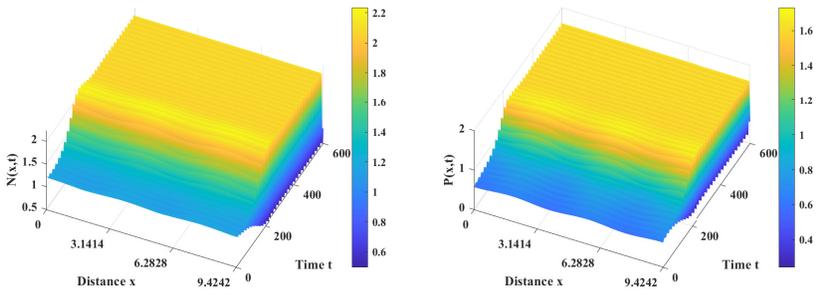

Figure 8. The positive equilibrium $E^*(1.1061, 0.6894)$ of (1) is unstable, and there exists stable spatially homogeneous periodic solutions for $(\tau_\varepsilon, d_{2\varepsilon}) = (2.0212, 0.022) \in D_2$.

When the parameters pass through the line T_2 from D_2 to D_3, A_3^+ and A_3^- are bifurcated from the boundary equilibria A_1 on the critical line T_2. In region D_3, system (16) has four equilibria A_0, A_1, and $A_3^{\pm}$. A_0, A_1 are unstable, and $A_3^{\pm}$ are stable. It means that the positive equilibrium of system (1) is unstable, the spatially homogeneous periodic solution is unstable, while there are two stable spatially inhomogeneous periodic solutions.

As the parameters pass through the line L_2 from D_3 to D_4, $A_2^{\pm}$ are bifurcated from the boundary equilibria A_0 on the critical line L_2. In region D_4, there are six equilibria: A_0, A_1, $A_2^{\pm}$, and $A_3^{\pm}$, where $A_3^{\pm}$ are stable and the rest equilibria are unstable. It means that two unstable spatially inhomogeneous steady-state solutions of system (1) appear, and the rest is the same as in D_3. When $(\tau_\varepsilon, d_{2\varepsilon}) = (0.0212, -0.001)$ lies in region D_4, Fig. 9 shows the existence of two stable spatially inhomogeneous periodic solutions for the initial values $N_0(x, t) = 1.2 \mp 0.01 \cos(5x/3)$ and $P_0(x, t) = 0.6 \pm 0.01 \cos(5x/3)$.

As the parameters pass through the line T_1 from D_4 to D_5, $A_3^{\pm}$ disappear on the critical line T_1 through pitchfork bifurcation. In region D_5, there are four equilibria: A_0, A_1, and $A_2^{\pm}$, where $A_2^{\pm}$ are stable, and the rest equilibria are unstable. It means that the positive equilibrium and the spatially homogeneous periodic solution of system (1) are unstable, while two spatially inhomogeneous steady-state solutions are stable.

When the parameters $(\tau_\varepsilon, d_{2\varepsilon})$ finally enter region D_6 from region D_5, A_1 disappears on the critical line L_1 through pitchfork bifurcation. In region D_6, there are three
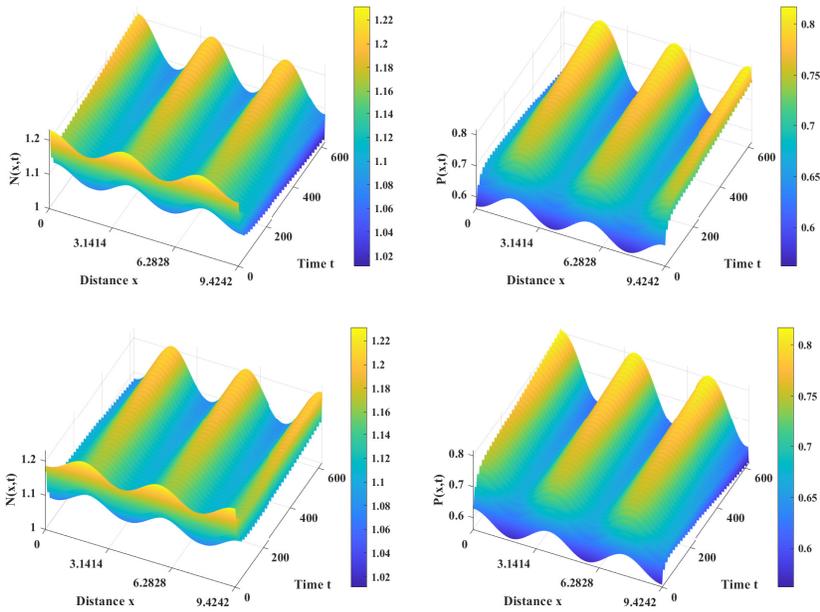
Figure 9. Two stable spatially inhomogeneous periodic solution for $(\tau_\varepsilon, d_{2\varepsilon}) = (0.0212, -0.001) \in D_4$.
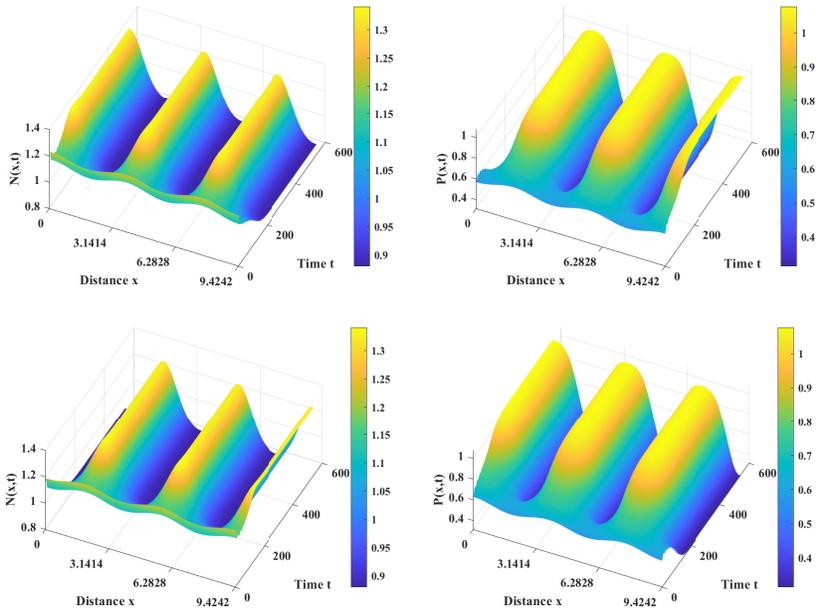

Figure 10. Two stable spatially inhomogeneous steady-state solutions appear for $(\tau_\varepsilon, d_{2\varepsilon}) = (-1.9788, -0.008) \in D_6$.

equilibria: A_0 and $A_2^{\pm}$, where $A_2^{\pm}$ are stable, and A_0 is unstable. It means that the spatially homogeneous periodic solution disappear, while the positive equilibrium of system (1) is unstable and two spatially inhomogeneous steady-state solutions are still stable. For $(\tau_\varepsilon, d_{2\varepsilon}) = (-1.9788, -0.008) \in D_6$, Fig. 10 shows the existence of two stable spatially inhomogeneous steady-state solutions with the initial values $N_0(x, t) = 1.2 \mp 0.01 \cos(5x/3)$ and $P_0(x, t) = 0.6 \pm 0.01 \cos(5x/3)$.

5 Conclusion

In this paper, we investigate the spatiotemporal dynamics of a diffusive nutrient-phytoplankton model with the effect of toxic chemicals released by phytoplankton and delayed nutrient recycling. Firstly, we analyze the stability of positive equilibrium and diffusion-driven instability of the nondelayed system, and we give the conditions for the stability and Turing instability. We also reveal the effect of nutrient recycling delay on our model. When the strength of k is high, the delay will not destabilize the positive equilibrium, and Hopf bifurcation will not occur. When the strength of k is low, Hopf bifurcation induced by delay can be observed. We find that the strength of k plays an important role in Hopf bifurcation. The results can help to understand the periodic outbreak of algae bloom. If we decrease θ to 0 and keep the other parameters the same, it turns out that neither Turing instability nor Hopf bifurcation will occur. It tells that in the absence of toxic effects, the distribution of phytoplankton remains homogeneous in spite of spatial movements of nutrient and phytoplankton. However, the presence of toxic effect makes phytoplankton distribution inhomogeneous in space induced by Turing instability and phytoplankton oscillation in time caused by delay-induced Hopf bifurcation.

To reveal the spatiotemporal dynamics induced by spatial diffusion and time delay, Turing–Hopf bifurcation analysis is carried out. We derive the normal form of Turing–Hopf bifurcation and obtain the dynamics classification near Turing–Hopf bifurcation. The parameter plane near Turing–Hopf bifurcation point can be de divided into six regions, and for each region, the dynamics are obtained clearly. When the parameters $(\tau_\varepsilon, d_{2\varepsilon})$ is in region D_1, the positive equilibrium is asymptotically stable. In D_2, there is a stable spatially homogeneous periodic solution. In D_3, two stable spatially inhomogeneous periodic solutions appear. When the parameters $(\tau_\varepsilon, d_{2\varepsilon})$ is in region D_4 and D_5, the stability of two spatially inhomogeneous steady-state solutions changes from unstable to stable. When $(\tau_\varepsilon, d_{2\varepsilon})$ enter D_6, the spatially homogeneous periodic solution disappears.

Although there have been many literature on models for interacting nutrient phytoplankton systems with toxic effects or nutrient recycling, the model we considered in this paper are different from the previous models. Chakraborty et al. [7] investigated a nutrient-phytoplankton system with toxic effect on phytoplankton, but they did not consider the effect of nutrient recycling. They focus on the effect of toxicity level on the spatial distribution. Singh et al. [25] took B–D-type response function to express the biomass conversion of nutrient, and they considered time delay not in nutrient recycling but in toxin liberation. They considered Turing and Hopf bifurcation, and they

demonstrated spatiotemporal dynamics by numerical simulation. Chakraborty et al. [6] considered such a model without diffusion and delay. They mainly discussed the dynamical behaviours by varying the toxin liberation rate and displayed phenomena from simple cyclical blooms to irregular chaotic blooms. In the previous work, Turing or Hopf bifurcation was investigated. Spatiotemporal dynamics in nutrient phytoplankton systems were obtained mainly by numerical simulations [7, 25], but not through Turing–Hopf bifurcation analysis. Different from the previous work, we focus on the joint effect of spatial diffusion and nutrient recycling delay through Turing–Hopf bifurcation analysis. Using Turing–Hopf bifurcation analysis, we can easily qualitatively classify dynamical behaviours on a two-parameter plane and understand the combined effects of diffusion and delay on nutrient and phytoplankton interactions.

In this paper, we incorporate a discrete delay to model the nutrient recycling. In fact, the dead plankton move during the recycling process, and they have not been at the same point in space at previous times. Thus, incorporating a nonlocal delay to model the process is more reasonable. There have been some studies on predator-prey or population systems incorporating nonlocal delays on a infinite or finite domain [11, 28]. We leave this for future investigation.

Appendix

The coefficient vectors $F_{y_i(\theta)z_j}$, F_{mnk} presented in normal form (13) can be obtained by using the following calculation formulas:

$$F_{y_1(0)z_1} = 2(F_{uu} + q_1 F_{uv}), \qquad F_{y_1(-1)z_1} = 0,$$
$$F_{y_1(0)z_2} = 2(F_{uu} + p_1 F_{uv}), \qquad F_{y_1(-1)z_2} = 0,$$
$$F_{y_2(0)z_1} = 2F_{uv}, \qquad F_{y_2(-1)z_1} = 0,$$
$$F_{y_2(0)z_2} = 2F_{uv}, \qquad F_{y_2(-1)z_2} = 0,$$
$$F_{200} = q_1^2 F_{vv} + 2q_1 F_{uv}, \qquad F_{002} = p_1^2 F_{vv} + 2p_1 F_{uv},$$
$$F_{110} = 2\big[q_1^2 F_{vv} + F_{uv}(q_1 + \bar{q}_1)\big], \qquad F_{020} = \overline{F_{200}},$$
$$F_{101} = 2\big[p_1 q_1 F_{vv} + F_{uv}(p_1 + q_1)\big], \qquad F_{011} = \overline{F_{101}},$$
$$F_{210} = 3F_{vvv}q_1^2\bar{q}_1, \qquad F_{111} = 6F_{vvv}q_1\bar{q}_1 p_1,$$
$$F_{102} = 3F_{vvv}q_1 p_1^2, \qquad F_{003} = F_{vvv}p_1^3,$$

where

$$F_{uv} = \begin{pmatrix} -b \\ c \end{pmatrix}, \qquad F_{vv} = \begin{pmatrix} 0 \\ -\frac{2\theta\mu^2(\mu^2-3P^{*2})}{(\mu^2+P^{*2})^3} \end{pmatrix},$$
$$F_{vvv} = \begin{pmatrix} 0 \\ \frac{24\theta P^*\mu^2(\mu^2-P^{*2})}{(\mu^2+P^{*2})^4} \end{pmatrix}.$$

References

1. Q. An, W. Jiang, Spatiotemporal attractors generated by the Turing-Hopf bifurcation in a time-delayed reaction-diffusion system, *Discrete Contin. Dyn. Syst., Ser. B*, **24**(2):487–510, 2019, `https://doi.org/10.3934/DCDSB.2018183`.

2. D.M. Anderson, Turning back the harmful red tide, *Nature*, **388**(6642):513–514, 1997, `https://doi.org/10.1038/41415`.

3. D.M. Anderson, P. Hoagland, Y. Kaoru, A.W. White, Estimated annual economic impacts from harmful algal blooms (HABs) in the United States, 2000, `https://doi.org/10.1575/1912/96`.

4. E. Beretta, G.I. Bischi, F. Solimano, Stability in chemostat equations with delayed nutrient recycling, *J. Math. Biol.*, **28**(1):99–111, 1990, `https://doi.org/10.1007/BF00171521`.

5. S. Busenberg, S.K. Kumar, P. Austin, G. Wake, The dynamics of a model of a plankton-nutrient interaction, *Bull. Math. Biol.*, **52**(5):677–696, 1990, `https://doi.org/10.1007/bf02462105`.

6. S. Chakraborty, S. Chatterjee, E. Venturino, J. Chattopadhyay, Recurring plankton bloom dynamics modeled via toxin-producing phytoplankton, *J. Biol. Phys.*, **33**(4):271–290, 2007, `https://doi.org/10.1007/s10867-008-9066-3`.

7. S. Chakraborty, P.K. Tiwari, A.K. Misra, J. Chattopadhyay, Spatial dynamics of a nutrient-phytoplankton system with toxic effect on phytoplankton, *Math. Biosci.*, **264**:94–100, 2015, `https://doi.org/10.1016/j.mbs.2015.03.010`.

8. J. Chattopadhayay, R.R. Sarkarw, S. Mandalw, Toxin-producing plankton may act as a biological control for planktonic blooms-field study and mathematical modelling, *J. Theor. Biol.*, **215**(3):333–344, 2002, `https://doi.org/10.1006/jtbi.2001.2510`.

9. C. Dai, M. Zhao, H. Yu, Dynamics induced by delay in a nutrient-phytoplankton model with diffusion, *Ecol. Complex.*, **26**:29–36, 2016, `https://doi.org/10.1016/j.ecocom.2016.03.001`.

10. J. Duinker, G. Wefer, Das CO_2-Problem und die Rolle des Ozeans, *Naturwissenschaften*, **81**:237–242, 1994, `https://doi.org/10.1007/BF01131574`.

11. S.A. Gourley, N.F. Britton, A predator-prey reaction-diffusion system with nonlocal effects, *J. Math. Biol.*, **34**:297–333, 1996, `https://doi.org/10.1007/bf00160498`.

12. J. Guckenheimer, P. Holmes, *Nonlinear Oscillations, Dynamical Systems, and Bifurcations of Vector Fields*, Springer, New York, 1983, `https://doi.org/10.1063/1.2814774`.

13. X.Z. He, S.G. Ruan, Global stability in chemostat-type plankton models with delayed nutrient recycling, *J. Math. Biol.*, **37**:253–271, 1998, `https://doi.org/10.1007/s002850050128`.

14. A. Huppert, B. Blasius, L. Stone, A model of phytoplankton blooms, *Am. Nat.*, **159**(2):156–171, 2002, `https://doi.org/10.1086/324789`.

15. S.J. Jang, J. Baglama, Nutrient-plankton models with nutrient recycling, *Comput. Math. Appl.*, **49**(2–3):375–387, 2005, `https://doi.org/10.1016/j.camwa.2004.03.013`.

16. J. Ji, L. Wang, Bifurcation and stability analysis for a nutrient-phytoplankton model with toxic effects, *Discrete Contin. Dyn. Syst., Ser. S*, **13**(11):3073–3081, 2020, `https://doi.org/10.3934/dcdss.2020135`.

17. Z. Jiang, M. Jie, Bifurcation control of a minimal model of marine plankton interaction with multiple delays, *Math. Model. Nat. Pheno.*, **16**(1):16, 2021, `https://doi.org/10.1051/mmnp/2021013`.

18. K.I. Keating, Allelopathic influence on blue-green bloom sequence in a eutrophic lake, *Science*, **196**(4292):885–887, 1977, `https://doi.org/10.1126/science.196.4292.885`.

19. R.M. Nisbet, W.S.C. Gurney, Model of material cycling in a closed ecosystem, *Nature*, **264**(5587):633–634, 1976, `https://doi.org/10.1038/264633a0`.

20. G.A. Riley, H.M. Stommel, D.F. Bumpus, *Quantitative Ecology of the Plankton of the Western North Atlantic*, Bull. Bingham Oceanogr. Collect., Vol. 12, Bingham Oceanographic Laboratory, 1949.

21. S. Ruan, J. Wei, On the zeros of transcendental functions with applications to stability of delay differential equations with two delays, *Dyn. Contin. Discrete Impuls. Syst., Ser. A, Math. Anal.*, **10**(6):863–874, 2003.

22. S.G. Ruan, Diffusion-driven instability in the gierer-meinhardt model of morphogenesis, *Nat. Resour. Model.*, **11**(2):131–141, 1998, `https://doi.org/10.1111/j.1939-7445.1998.tb00304.x`.

23. S.G. Ruan, Turing instability and travelling waves in diffusive plankton models with delayed nutrient recycling, *IMA J. Appl. Math.*, **61**(1):15–32, 1998, `https://doi.org/10.1093/imamat/61.1.15`.

24. L.E. Schmidt, P.J. Hansen, Allelopathy in the prymnesiophyte *Chrysochromulina* polylepis: Effect of cell concentration, growth phase and pH, *Mar. Ecol. Prog. Ser.*, **216**:67–81, 2001, `https://doi.org/10.3354/meps216067`.

25. R. Singh, S. Kumar Tiwari, A. Ojha, N.K. Thakur, Dynamical study of nutrient-phytoplankton model with toxicity: Effect of diffusion and time delay, *Math. Meth. Appl. Sci.*, **46**(1):490–509, 2023, `https://doi.org/10.1002/mma.8523`.

26. Y. Song, H. Jiang, Y. Yuan, Turing-Hopf bifurcation in the reaction-diffusion system with delay and application to a diffusive predator-prey model, *J. Appl. Anal. Comput.*, **9**(3):1132–1164, 2019, `https://doi.org/10.11948/2156-907X.20190015`.

27. Y.L. Song, X.F. Zou, Bifurcation analysis of a diffusive ratio-dependent predator-prey model, *Nonlinear Dyn.*, **78**(1):49–70, 2014, `https://doi.org/10.1007/s11071-014-1421-2`.

28. Y. Tao, S.A. Campbell, F.J. Poulin, Dynamics of a diffusive nutrient-phytoplankton-zooplankton model with spatio-temporal delay, *SIAM J. Appl. Math.*, **81**(6):2405–2432, 2021, `https://doi.org/10.1137/20M1378065`.

29. C. Tian, L. Zhang, Delay-driven irregular spatiotemporal patterns in a plankton system, *Phys. Rev. E*, **88**(1):012713, 2013, `https://doi.org/10.1103/PhysRevE.88.012713`.

30. Y. Wang, H.B. Wang, W.H. Jiang, Stability switches and global Hopf bifurcation in a nutrient-plankton model, *Nonlinear Dyn.*, **78**(2):981–994, 2014, `https://doi.org/10.1007/s11071-014-1491-1`.

31. A.J. Windust, J.L.C. Wright, J.L. Mclachlan, The effects of the diarrhetic shellfish poisoning toxins, okadaic acid, and dinophysistoxin-1, on the growth of microalgae, *Mar. Biol.*, **126**(1):19–25, 1996, `https://doi.org/10.1007/BF00571373`.

32. C.C. Wu, The spreading speed for a predator–prey model with one predator and two preys, *Appl. Math. Lett.*, **91**:9–14, 2018, `https://doi.org/10.1016/j.aml.2018.11.022`.

33. J. Wu, *Theory and Application of Partial Functional Differential Equations*, Springer, New York, 1996, `https://doi.org/10.1007/978-1-4612-4050-1`.

34. J.T. Zhao, J.J. Wei, Dynamics in a diffusive plankton system with delay and toxic substances effect, *Nonlinear Anal., Real World Appl.*, **22**:66–83, 2015, `https://doi.org/10.1016/j.nonrwa.2014.07.010`.

35. K. Zhuang, Y. Li, B. Gong, Stability switches and Hopf bifurcation induced by nutrient recycling delay in a reaction-diffusion nutrient-phytoplankton model, *Complexity*, **2021**: 7943788, 2021, `https://doi.org/10.1155/2021/7943788`.